Cutaneous Feedback of Fingertip Deformation and Vibration for Palpation in Robotic Surgery

Claudio Pacchierotti, Domenico Prattichizzo, *Senior Member, IEEE,*
and Katherine J. Kuchenbecker, *Member, IEEE*

***Abstract*—Despite its expected clinical benefits, current teleoperated surgical robots do not provide the surgeon with haptic feedback largely because grounded forces can destabilize the system's closed-loop controller. This article presents an alternative approach that enables the surgeon to feel fingertip contact deformations and vibrations while guaranteeing the teleoperator's stability. We implemented our cutaneous feedback solution on an Intuitive Surgical da Vinci Standard robot by mounting a SynTouch BioTac tactile sensor to the distal end of a surgical instrument and a custom cutaneous display to the corresponding master controller. As the user probes the remote environment, the contact deformations, DC pressure, and AC pressure (vibrations) sensed by the BioTac are directly mapped to input commands for the cutaneous device's motors using a model-free algorithm based on look-up tables. The cutaneous display continually moves, tilts, and vibrates a flat plate at the operator's fingertip to optimally reproduce the tactile sensations experienced by the BioTac. We tested the proposed approach by having eighteen subjects use the augmented da Vinci robot to palpate a heart model with no haptic feedback, only deformation feedback, and deformation plus vibration feedback. Fingertip deformation feedback significantly improved palpation performance by reducing the task completion time, the pressure exerted on the heart model, and the subject's absolute error in detecting the orientation of the embedded plastic stick. Vibration feedback significantly improved palpation performance only for the seven subjects who dragged the BioTac across the model, rather than pressing straight into it.**

I. Introduction

TELEOROBOTIC surgical systems involve a slave robot, which interacts with the patient, and a master console, operated by the human surgeon. The slave robot reproduces the hand movements of the surgeon, who in turn needs to observe the operative environment with which the robot is interacting. If the surgeon receives sufficient information about the slave system and the operative environment, he or she will feel present at the operative site, a condition commonly referred to as telepresence [1], [2]. The strength of the telepresence illusion depends on the type and quality of information that flows from the operating table to the surgeon. Visual feedback is already available in commercial robotic surgery systems (e.g., the Intuitive Surgical da Vinci Si), but current surgical robots have very limited haptic feedback. This omission is mainly due to the negative effect that haptic force feedback has on the stability of the teleoperation loop; outputting grounded forces with the master console can lead to undesired oscillations of the system, which interfere with the surgery and may be dangerous for the patient [3], [4]. However, haptic feedback is still widely believed to be valuable for teleoperated surgical procedures [5], [6], [7], [8], [9]. It has been shown to enhance surgeon performance in a wide range of applications including microneedle positioning [10], telerobotic catheter insertion [11], suturing simulation [12], cardiothoracic procedures [13], and cell injection [14]. Its benefits typically include increased manipulation accuracy, increased perception accuracy, decreased completion time, and decreased peak and mean force applied to the remote environment [15], [16], [17], [18], [4], [19], [20].

Given the expected benefits of haptic feedback and the challenges of stable implementation, many researchers have turned to sensory substitution techniques, wherein force information is presented via an alternative feedback channel, such as vibrotactile [21], auditory [22], or visual cues [23]. Because no haptic forces are displayed to the operating surgeon, sensory substitution techniques make teleoperation systems intrinsically stable [4], [18], [20]. However, although the stability of the system is guaranteed, the provided stimuli differ substantially from the ones being substituted (e.g., a beep sound instead of force feedback). Therefore, sensory substitution often shows performance inferior to that achieved with unaltered force feedback [4], [20].

Cutaneous feedback has recently received great attention from researchers looking for an alternative to sensory substitution of force feedback. Cutaneous stimuli are detected by mechanoreceptors in the skin, enabling humans to recognize the local properties of objects such as shape, edges, and texture. Cutaneous perception for exploration and manipulation principally relies on measures of the location, intensity, direction, and timing of contact forces on the fingertips [24], [25]. Delivering this type of haptic cues to the surgeon's skin has been proved to convey rich information and does not affect

C. Pacchierotti is with the Dept. of Information Engineering and Mathematics, University of Siena, Siena, Italy, with the Dept. of Advanced Robotics, Istituto Italiano di Tecnologia, Genova, Italy, and with the Depts. of Mechanical Engineering & Applied Mechanics and Computer & Information Science, GRASP Laboratory, University of Pennsylvania, Philadelphia, PA, USA. E-mail: pacchierotti@dii.unisi.it.

D. Prattichizzo is with the Dept. of Information Engineering and Mathematics, University of Siena, Siena, Italy and with the Dept. of Advanced Robotics, Istituto Italiano di Tecnologia, Genova, Italy. E-mail: prattichizzo@dii.unisi.it.

K. J. Kuchenbecker is with the Depts. of Mechanical Engineering & Applied Mechanics and Computer & Information Science, GRASP Laboratory, University of Pennsylvania, Philadelphia, PA, USA.
E-mail: kuchenbe@seas.upenn.edu.

The research leading to these results has received funding from the European Union Seventh Framework Programme FP7/2007-2013 under grant agreement n°601165 of the project "WEARHAP - WEARable HAPtics for humans and robots."

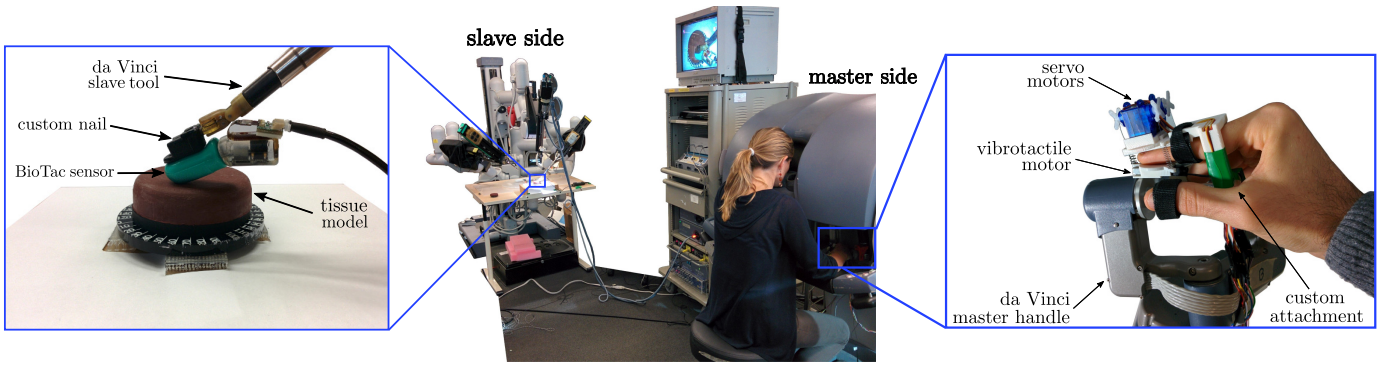

Fig. 1. System setup. A BioTac tactile sensor (*left*) measures contact deformations and vibrations at the operating table, and a custom cutaneous feedback device (*right*) applies those deformations and vibrations to the surgeon's fingertip. The BioTac is attached to a da Vinci slave tool, and the cutaneous feedback device is attached to the robot's corresponding master controller. The BioTac follows the motions of the operator's finger.

the stability of the teleoperation system [4], [20], [26]. Many cutaneous feedback techniques for teleoperation have been presented in the literature, exploiting the different types of cutaneous stimuli that mechanoreceptors in the skin can detect. For example Prattichizzo *et al.* [4] showed that cutaneous feedback provided by a moving platform is more effective than sensory substitution via visual feedback in a needle insertion task, and Meli et al. [20] found the same type of cutaneous feedback more effective than sensory substitution via either visual or auditory feedback in a pick-and-place task similar to the da Vinci Skills Simulator's Pegboard task. Similar to the moving platforms mentioned above, pneumatic balloon-based systems are another popular approach to relaying contact force via cutaneous feedback. King *et al.* [27], [28] developed a modular pneumatic cutaneous feedback system to improve the performance of the da Vinci surgical system. The system includes piezoresistive force sensors mounted on the gripping surfaces of a robotic tool and two pneumatic balloon-array tactile displays mounted on the robot's master console. More recently, Li *et al.* [29] extended this approach to three fingers, presenting a compact pneumatic system for robot-assisted palpation. It simulates tissue stiffness by changing the pressure in three balloons placed on the index, middle, and ring fingers. Stanley and Okamura [30] combined pneumatics and particle jamming to simultaneously control the shape and mechanical properties of a cutaneous display. The system includes a hollow silicone membrane molded into an array of thin cells. Each cell is filled with coffee grounds such that adjusting the vacuum level in any individual cell rapidly switches it between flexible and rigid states. Li *et al.* [31] used granular jamming stiffness feedback actuators for simulating multi-fingered tissue palpation procedures in traditional and in robot-assisted minimally invasive surgery. Soft tissue stiffness is simulated by changing the stiffness property of the actuator during palpation.

Another line of research has focused on cutaneous feedback of tactile vibrations, which are caused by changes in the slave end-effector's contact state. Kontarinis and Howe presented the first evidence of the benefits of this approach [32]. The system created by McMahan *et al.* [26] for the Intuitive da Vinci robot lets the surgeon feel left and right instrument vibrations in real time without destabilizing the closed-loop controller. 114 surgeons and non-surgeons tested this system in dry-lab manipulation tasks and expressed a significant preference for the inclusion of cutaneous feedback of instrument vibrations [33]. Prattichizzo *et al.* call this overall approach *sensory subtraction*, in contrast to *sensory substitution*, as it subtracts the destabilizing kinesthetic part of the haptic interaction to leave only cutaneous cues.

Inspired by the success of sensory subtraction, this paper presents a novel cutaneous feedback system for the da Vinci surgical robot, as shown in Fig. 1. It provides cutaneous feedback of fingertip contact deformation and vibration to the surgeon while guaranteeing the stability and safety of the controller. The system is composed of a BioTac tactile sensor, mounted to one of the robot's slave tools, and a custom cutaneous display, attached to the corresponding master controller. Contact deformations and vibrations sensed by the BioTac are directly mapped to input commands for the cutaneous device's motors using a model-free algorithm based on look-up tables. To our knowledge, a BioTac sensor has not previously been added to a surgical robot, nor have fingertip deformations and vibrations been combined. A preliminary version of the deformation part of the algorithm was presented in [34], and an evaluation of its fidelity at rendering pre-recorded contacts with a planar surface was presented in [35].

This article significantly extends our prior work by adding sensing and actuation of vibrations, incorporating the system into a da Vinci robot, and testing the utility of the provided cutaneous cues in a clinically relevant palpation task. Because palpation technology is not yet commercially available, robotic minimally invasive systems are currently being used in procedures that can be completed without palpation. However, being able to palpate the patient's tissue during surgery would enable the operating surgeon to feel exactly where tumors are located and to therefore tailor the surgery to the patient's current disease state, trying to remove all of the cancer while sparing as much of the patient's healthy tissue as possible. In this way, palpation could enable surgeons to deliver better care in procedures they are already performing robotically, and it could also broaden the range of operations that can be done with a minimally invasive robotic surgical system.

Sec. II presents the system we created, and Sec. III describes the algorithm that maps the deformations and vibrations registered by the tactile sensor to the input commands for the cutaneous device's motors. Sec. IV describes the experiment that we ran to evaluate the presented system, wherein human subjects palpated a simulated tissue model. Secs. V and VI present and discuss the results of this experiment, respectively. We conclude the article in Sec. VII and discuss avenues for future work in Sec. VIII.

II. Haptic Sensing and Actuation

The SynTouch BioTac tactile sensor mimics the physical properties and sensory capabilities of the human fingertip [36]. As shown in the left panel of Fig. 1 and in Fig. 2a, it consists of three complementary sensing systems (deformation, internal fluid pressure, and temperature) integrated into a single package. Contact forces deform the elastic skin and the underlying conductive fluid, changing the impedances of 19 electrodes distributed over the surface of the rigid core. The DC pressure of the conductive fluid is measured by a hydro-acoustic pressure sensor, which also detects the AC pressure changes caused by transient contacts such as textures. The BioTac can register changes in its fluid pressure as small as 37 Pa and changes in vibrations as small as 0.4 Pa. As shown in Fig. 1, we attached the BioTac sensor to a da Vinci Standard electrocautery spatula tool through a custom plastic fingernail that replaces the nail provided by the BioTac's manufacturer. We selected the electrocautery spatula tool solely for its flat shape; we did not use its cautery function. While this sensing arrangement is bulky and non-sterilizable, it could be redesigned and miniaturized for use in minimally invasive robotic surgery if the information it provides was found to benefit the surgeon; see [37] and Sec. VIII for ideas on updating the BioTac for surgical use.

The cutaneous display employed in this work is shown in the right panel of Fig. 1 and in Fig. 2b. It is an augmented version of the 3-DoF fingertip device presented in [19]. The device frame houses three servo motors and is rigidly clamped to the tip of the two-fingered grasping interface of the right da Vinci master controller. The operator's thumb and middle finger are inserted into the da Vinci straps, and the operator's index finger is placed inside the cutaneous feedback device, which fastens with a strap between the PIP and DIP joints. Foam covered with a thin layer of adhesive cushions the back of the fingertip and further immobilizes it within the device. A mobile platform holding one vibrotactile motor is suspended beneath the operator's fingertip by three cables. Compression springs around the cables hold the mobile platform in a reference configuration away from the fingertip. By controlling the cable lengths, the servos orient and translate the mobile platform in three-dimensional space to apply planar deformations to the fingertip, while the vibrotactile motor conveys fingertip vibrations. In some configurations, the platform does not contact the fingertip, enabling the device to portray the making and breaking of contact in a manner similar to the Contact Location Display [38]. The servo motors used in our prototype are Sub-Micro Servo 3.7 g motors (Pololu Corporation, USA), which

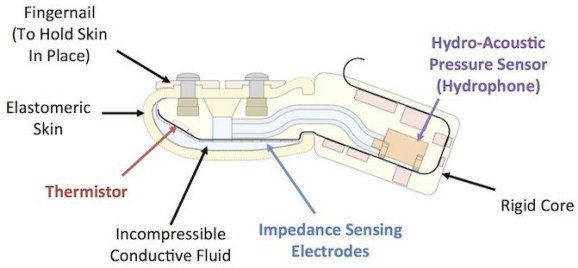

(a) Cross-section diagram of the BioTac sensor (picture courtesy of SynTouch LLC)

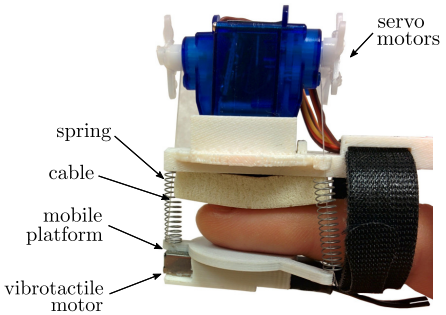

(b) Custom 3-DoF cutaneous feedback device

Fig. 2. Fingertip sensing and actuation. (a) Contact forces deform the BioTac's skin and conductive fluid, changing the impedances of 19 electrodes distributed over the surface of the rigid core. Vibrations in the skin propagate through the fluid and are detected by the hydro-acoustic pressure sensor, which also measures the fluid's DC pressure. (b) The cutaneous feedback device includes three servo motors on a frame fixed to the back of the user's finger. Three cables with concentric springs suspend a flat mobile platform holding one vibrotactile motor beneath the fingertip. By controlling the cable lengths, the servos move the mobile platform in three-dimensional space to apply contact deformations to the fingertip, while the vibrotactile motor conveys fingertip vibrations.

are position controlled and can each exert up to 39 N·mm torque. Our vibrotactile motor is a Forcereactor short-vibration feedback motor (Alps Electric, Japan). A brief video showing the device can be found at http://goo.gl/orylg2. While this actuation arrangement is quite bulky, it could be redesigned and miniaturized taking into account ergonomic and comfort factors [39], [40], [41], [42].

III. Mapping Sensed Data to Motor Commands

Our goal is to enable the user to perceive, through the fingertip cutaneous device, the deformations and vibrations experienced by the BioTac as it interacts with the operative environment during a clinically relevant task such as palpation. In other words, we aim to find a good many-to-few mapping between the rich sensory information measured by the BioTac and the limited actuation capabilities of the fingertip cutaneous device. This problem of mapping cutaneous readings to cutaneous actuation pertains to any such feedback system, not just our particular prototype, so we developed a general solution.

Because our focus is on sensing deformations and vibrations, we consider the 19 electrode impedance readings, the DC output of the hydro-acoustic pressure sensor, and the AC output of the same pressure sensor. The BioTac registers the electrode data and DC pressure at 100 Hz and the AC pressure at 2200 Hz. All of these quantities are sensed with a precision

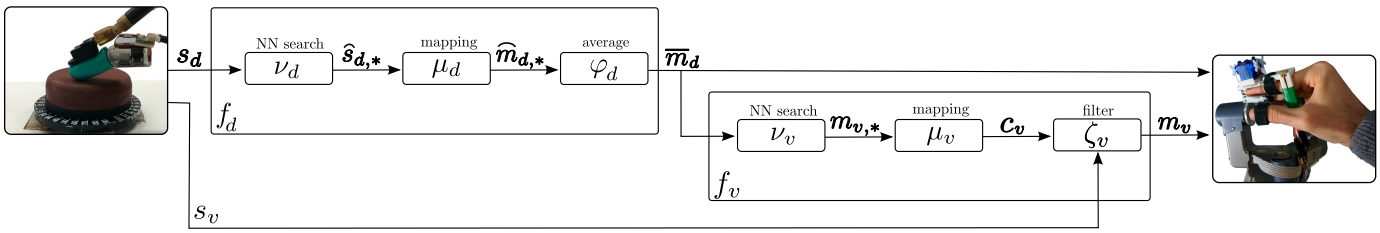

Fig. 3. Mapping algorithm. The BioTac registers a tactile sensation $[\boldsymbol{s_d} \quad s_v]^T$ at the remote environment. Function $\nu_d(\cdot)$ looks for the eight closest points contained in $\mathbb{S}_{d,*}$, recorded during data collection. These points are then mapped by $\mu_d(\cdot)$ to their corresponding motor angle triplets. Function $\varphi_d(\cdot)$ averages those points to find the angle triplet $\overline{\boldsymbol{m}}_{\boldsymbol{d}}$ to be actuated by the servos. Once the platform configuration is defined, function $\nu_v(\cdot)$ looks for the closest platform configuration contained in $\mathbb{M}_{v,*}$, recorded during data collection, and retrieves the corresponding vibration transfer function. Finally, $\zeta_v(\cdot)$ filters the vibrations sensed by the BioTac accordingly.

of 12 bits. Let $\boldsymbol{s_d(j)} \in \mathbb{S}_d = \{(s_{d,1}(j), \ldots, s_{d,20}(j)) \in \mathbb{Z}^{20} : 0 \leq s_{d,i}(j) \leq 4095\}$ be a vector containing the electrode and DC pressure values sensed at instant j. Let $s_v(k) \in \mathbb{S}_v = \{s_v(k) \in \mathbb{Z} : 0 \leq s_v(k) \leq 4095\}$ be the AC pressure sensed at instant k. In contrast, our cutaneous feedback device uses three position-controlled motors and one vibrotactile motor. Let $\boldsymbol{m_d(j)} \in \mathbb{M}_d = \{(m_{d,1}(j), m_{d,2}(j), m_{d,3}(j)) \in \mathbb{R}^3 : 30° \leq m_{d,i}(j) < 200°\}$ be a vector containing the commanded angles for the three position-controlled motors at instant j, and $m_v(k) \in \mathbb{M}_v = \{m_v(k) \in \mathbb{R} : -1 \leq m_v(k) \leq 1\}$ the commanded signal for the vibrotactile motor at instant k. Note that we are neglecting quantization in the motor position outputs for simplicity. To simplify the notation further, the sampling time indices j and k will be omitted from now on.

As summarized in Fig. 3, we developed a reliable way to map a given BioTac sensation, defined by $\boldsymbol{s_d}$ and s_v, to a congruent configuration of the mobile platform $\boldsymbol{m_d}$ and signal for the vibrotactile motor m_v. Rather than attempting to create an accurate mechanical model of the actuation and sensing systems from first principles, we solved this problem with a data-driven approach that uses look-up tables of fingertip deformation recordings vs. motor commands and vibration recordings vs. motor commands. Specifically, we placed the BioTac inside the cutaneous device and tested how the motion of the mobile platform affects the fingertip deformation and vibration readings, as described in Sec. III-A. During teleoperation these recorded data are used to map contact deformations sensed by the BioTac to input commands for the cutaneous device's servo motors, as detailed in Sec. III-B. Finally, Sec. III-C explains how vibrations sensed by the BioTac are mapped to input commands for the cutaneous device's vibrotactile motor.

A. Data Collection

As shown in Fig. 4, the BioTac was placed between the foam and the mobile platform, in the same way a human user would wear the device (compare with Fig. 2b), but with the cables lengthened to accommodate the custom nail. We then moved the mobile platform to a wide range of configurations and recorded the effect of each of these configurations on the BioTac, saving both the commanded servo motor angles $\boldsymbol{m_{d,*}}$ and the resulting effect on the tactile sensor's electrodes and DC pressure $\boldsymbol{s_{d,*}}$. Using a moderate step size of 5° yields $(\frac{200°-30°}{5°})^3 = 39304$ unique platform configurations.

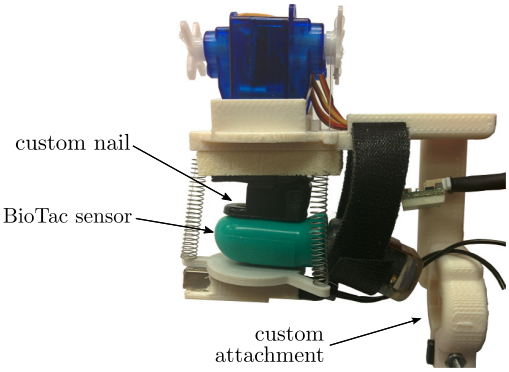

Fig. 4. Data collection. The BioTac was placed inside the cutaneous feedback device, and the platform was moved to 39304 different configurations. Servo motor inputs $\boldsymbol{m_{d,*}}$ and the resulting effect on the tactile sensor's electrodes and DC pressure $\boldsymbol{s_{d,*}}$ were recorded. For 4913 of these configurations, we also played a two-second-long swept sine wave (1 Hz – 1000 Hz) through the vibrotactile motor and registered its effect on the BioTac's pressure sensor $s_{v,*}$ (AC signals).

The platform was held in each configuration for 0.2 s, and the values gathered by the BioTac were arithmetically averaged. The mechanical coupling between the platform and the fingerpad changes dramatically over the workspace of the device. To understand how different platform configurations affect the way the BioTac feels vibrations, we also played a two-second-long swept sine wave (1 Hz – 1000 Hz) through the vibrotactile motor and registered its effect on the BioTac's AC pressure signal $s_{v,*}$. Due to their long duration, the swept-sinusoid tests were conducted at a subset of the configurations listed above, using a step size of 10°, which yields $(\frac{200°-30°}{10°})^3 = 4913$ unique platform configurations. Data collection lasted approximately 22 hours.

The collected data defines a look-up table of the fingertip deformations caused by motion of the mobile platform, and it enables us to evaluate the mapping function

$$\begin{aligned} &\mu_d : \mathbb{S}_{d,*} \rightarrow \mathbb{M}_{d,*}, \\ &\mu_d(\boldsymbol{s_{d,*}}) = \boldsymbol{m_{d,*}}, \end{aligned} \tag{1}$$

which links the BioTac's electrode and DC pressure readings to the corresponding tested servo motor inputs. Set $\mathbb{M}_{d,*} \subset \mathbb{M}_d$ contains all the angle triplets actuated during data collection, and $\mathbb{S}_{d,*} \subset \mathbb{S}_d$ contains all the resulting sensed values registered by the BioTac. Moreover, for the 4913 platform configurations tested with the swept sine wave,

we were also able to estimate the transfer function between the vibrations sensed by the BioTac and the swept sine wave played through the vibrotactile motor; this fitting was performed with the MATLAB function `tfest`, and each transfer function contained 6 poles and 6 zeros. We were then again able to define a look-up table of vibration recordings vs. motion of the mobile platform and evaluate the mapping function

$$\begin{aligned} &\mu_v : \mathbb{M}_{v,*} \rightarrow \mathbb{R}^{14}, \\ &\mu_v(\boldsymbol{m_{v,*}}) = \boldsymbol{c_v}, \end{aligned} \tag{2}$$

which links each of the 4913 tested platform configurations $\boldsymbol{m_{v,*}}$ to the corresponding transfer function's fourteen coefficients $\boldsymbol{c_v}$. Set $\mathbb{M}_{v,*} \subset \mathbb{M}_{d,*}$ contains the angle triplets tested with the swept sine wave during data collection.

B. From the BioTac to the Servo Motors

Given its 12-bit resolution, the BioTac can sense up to 4096^{20} ($\sim 1.77 \times 10^{72}$) different contact sensations through its electrodes and pressure sensor. However, our data collection tested only 39304 different platform configurations, which inevitably yields a mapping function $\mu_d(\cdot)$ that is defined for only a small subset of all the possible tactile sensations the BioTac can experience. For this reason, we cannot simply deploy the sensor in a random remote environment and expect its sensed points to be in the domain of our mapping function. Unfortunately, this problem cannot be fixed by reducing the angle step size during data collection. The shape of the platform and the limited degrees of freedom of the device will always couple the behavior of neighboring electrodes, so many tactile inputs that the BioTac can sense cannot be reached with the given device.

We thus need a function that maps a *generic* sensed point $\boldsymbol{s_d} \in \mathbb{S}_d$ to one in our mapping function's domain $\mathbb{S}_{d,*}$. We address this problem by looking for the n-points in our domain closest to the sensed one, thus defining

$$\begin{aligned} &\nu_d : \mathbb{S}_d \rightarrow \mathbb{S}_{d,*}^n, \\ &\nu_d(\boldsymbol{s_d}) = \begin{bmatrix} \boldsymbol{s_{d,*,1}} \\ \boldsymbol{s_{d,*,2}} \\ \vdots \\ \boldsymbol{s_{d,*,n}} \end{bmatrix} = \hat{\boldsymbol{s}}_{\boldsymbol{d,*}}, \end{aligned} \tag{3}$$

as the function that maps a generic point $\boldsymbol{s_d} \in \mathbb{S}_d$, sensed by the BioTac, to the n closest ones in $\mathbb{S}_{d,*}$. We implemented the nearest point search using the Approximate Nearest Neighbour (ANN) C++ library by Mount and Arya [43]. We use $n = 8$ because we previously found that retrieving the eight closest points provides a good trade-off between tactile output performance and computational load [35]. Distances were calculated using the 20-dimensional Euclidean distance metric. To evenly weight the twenty elements of the sensed data when computing the distance, we divided each component of $\boldsymbol{s_{d,*}}$ by the corresponding standard deviation observed during data collection, so that the standard deviation of each component of the vectors in $\mathbb{S}_{,*}$ becomes 1. The same operation was applied to $\boldsymbol{s_d}$ at run time.

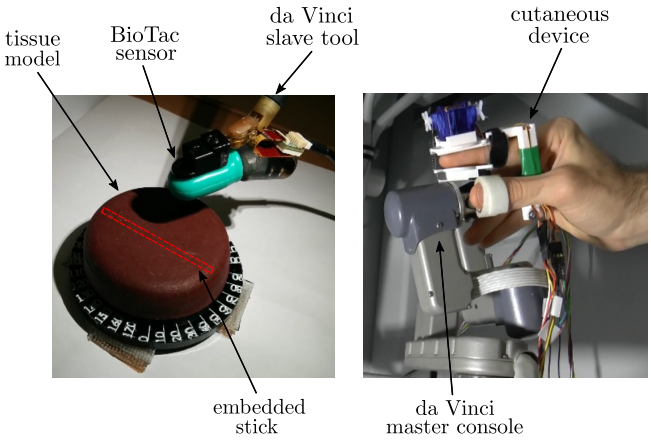

(a) Remote environment (b) Master console

Fig. 5. Experimental setup. The cutaneous feedback device is attached to the robot's right master controller, and the BioTac to the corresponding da Vinci tool, so that the BioTac mimics the motion and orientation of the operator's index finger. The remote environment is composed of a simulated heart soft tissue model with a plastic stick embedded at 1.5 mm from the surface. The orientation of the stick changes randomly at each repetition of the task.

We can now map the n points retrieved by $\nu_d(\cdot)$ to their corresponding motor angle triplets from data collection,

$$\begin{aligned} &\mu_d : \mathbb{S}_{d,*}^n \rightarrow \mathbb{M}_{d,*}^n, \\ &\mu_d(\hat{\boldsymbol{s}}_{\boldsymbol{d,*}}) = \mu_d \left(\begin{bmatrix} \boldsymbol{s_{d,*,1}} \\ \boldsymbol{s_{d,*,2}} \\ \vdots \\ \boldsymbol{s_{d,*,n}} \end{bmatrix} \right) = \begin{bmatrix} \mu_d(\boldsymbol{s_{d,*,1}}) \\ \mu_d(\boldsymbol{s_{d,*,2}}) \\ \vdots \\ \mu_d(\boldsymbol{s_{d,*,n}}) \end{bmatrix} = \\ &= \begin{bmatrix} \boldsymbol{m_{d,*,1}} \\ \boldsymbol{m_{d,*,2}} \\ \vdots \\ \boldsymbol{m_{d,*,n}} \end{bmatrix} = \widehat{\boldsymbol{m}}_{\boldsymbol{d,*}}, \end{aligned} \tag{4}$$

Finally, we can average $\widehat{\boldsymbol{m}}_{\boldsymbol{d,*}} \in \mathbb{M}_{d,*}^n$ to a single angle triplet for the servo motors as

$$\begin{aligned} &\varphi_d : \mathbb{M}_{d,*}^n \rightarrow \mathbb{M}_d, \\ &\varphi_d(\widehat{\boldsymbol{m}}_{\boldsymbol{d,*}}) = \varphi_d \left(\begin{bmatrix} \boldsymbol{m_{d,*,1}} \\ \boldsymbol{m_{d,*,2}} \\ \vdots \\ \boldsymbol{m_{d,*,n}} \end{bmatrix} \right) = \overline{\boldsymbol{m}}_{\boldsymbol{d}}, \end{aligned} \tag{5}$$

considering a simple inverse squared distance mean that weights angle triplets according to the inverse squared distance between the corresponding point in $\mathbb{S}_{d,*}$ and the one sensed by the BioTac [35]. Vector $\overline{\boldsymbol{m}}_{\boldsymbol{d}} \in \mathbb{M}_d$ is our final command for the servo motors at this time step.

C. From the BioTac to the Vibrotactile Motor

Data collection also tested how 4913 different platform configurations affect the transmission of vibrations from the vibrotactile motor to the BioTac's AC pressure sensor. This data collection set $\mathbb{M}_{v,*}$ is much smaller than $\mathbb{M}_d$, the set that contains the designated input for the servo motor $\overline{\boldsymbol{m}}_{\boldsymbol{d}}$. Similar to the methods of Sec. III-B, we address this problem by

looking for the platform configuration in $\mathbb{M}_{v,*}$ that is closest to $\overline{\boldsymbol{m}}_{\boldsymbol{d}}$, and thus define

$$\begin{aligned} &\nu_v : \mathbb{M}_d \rightarrow \mathbb{M}_{v,*}, \\ &\nu_v(\overline{\boldsymbol{m}}_{\boldsymbol{d}}) = \boldsymbol{m}_{\boldsymbol{v},*}, \end{aligned} \tag{6}$$

as the function that maps a generic platform configuration $\overline{\boldsymbol{m}}_{\boldsymbol{d}}$ to the closest one tested with the swept sine wave.

We can now retrieve the corresponding transfer function's coefficients, as defined in (2), and filter the vibration waveform sensed by the BioTac accordingly,

$$\begin{aligned} &\zeta_v : (\mathbb{S}_v, \mathbb{R}^{14}) \rightarrow \mathbb{M}_v, \\ &\zeta_v(s_v, \boldsymbol{c}_{\boldsymbol{v}}) = \zeta_v(s_v, \mu_v(\boldsymbol{m}_{\boldsymbol{v},*})) = m_v. \end{aligned} \tag{7}$$

This function filters the BioTac's sensed vibration to create a command suitable for the vibrotactile motor, taking into account how the present platform configuration affects the way vibrations propagate from the motor to the sensor. We filtered the signal using a floating-point implementation of an IIR filter [44]. Value m_v is our command for the vibrotactile motor at this time step.

IV. Experimental Evaluation

We evaluated the described haptic system by having human subjects carry out a palpation task using our augmented da Vinci robot. Figs. 1 and 5 show the experimental setup. The cutaneous feedback device is attached to the robot's right master controller, and the BioTac to the corresponding da Vinci tool, so that the BioTac follows the motion of the operator's index finger. The master and slave attachments are constructed so that the orientation of the BioTac always matches the orientation of the operator's index finger. The remote environment is composed of a simulated heart tissue model made from Ecoflex 0010 (Smooth-On Inc., USA) and brown dye. As shown in Fig. 6, a plastic stick with a circular cross section is embedded into the tissue model at 1.5 mm from the surface to simulate the presence of a calcified artery, following the methods of [45]. The stick is not visible from the outside. To minimize the utility of any incidental visual cues, the study used three identical copies of this heart model that were interchanged between trials.

Eighteen participants took part in the experiment, including 7 women and 11 men. Five of them had previous experience with haptic interfaces. None of the participants reported any deficiencies in their visual or haptic perception abilities, and all of them were right-hand dominant. The experimenter explained the procedures and spent about three minutes adjusting the setup to be comfortable before the subject began the experiment. Each subject then spent about two minutes practicing controlling the BioTac through the master console. Subjects consented to participate in this study under the University of Pennsylvania's Institutional Review Board protocol #820386.

The task consisted of exploring the tissue model to try to detect the orientation of the hidden plastic stick. As shown in Fig. 5, the tissue model was placed on a rounded plastic base with 36 ticks. The ticks indicate the 18 possible orientations of the hidden stick, reporting angles from 0° to 180°, with a step size of 10°. Subjects were asked to explore the tissue

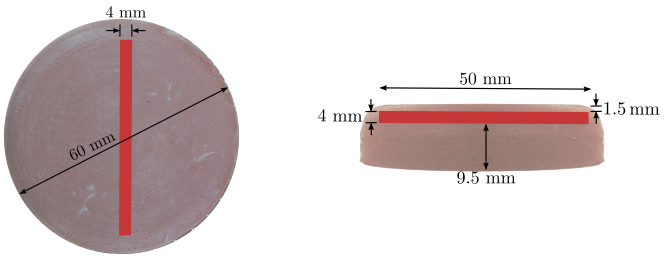

(a) Top view (b) Side view

Fig. 6. Simulated heart tissue model. The overall diameter and thickness of the model are 60 mm and 15 mm, respectively. A 4-mm-diameter plastic stick is embedded at a depth of 1.5 mm from the surface to mimic a calcified artery.

model and tell the experimenter the orientation of the stick. The task started when the BioTac touched the tissue model for the first time and ended when the subject told the experimenter the estimated orientation. Each participant performed twelve trials of the palpation task, with four repetitions for each of the following three feedback conditions:

- **Condition N:** no haptic feedback
- **Condition S:** cutaneous feedback of fingertip deformation provided by the servo motors
- **Condition SV:** cutaneous feedback of fingertip deformation provided by the servo motors plus cutaneous feedback of fingertip vibration by the vibrotactile motor

In condition N, the servo and vibrotactile motors were not active, and the mobile platform was always in contact with the subject's fingertip. In condition S, the servo motors moved the mobile platform as described in Sec. III-B, and the vibrotactile motor was not active. In condition SV, the servo motors moved the mobile platform as in condition S, and the vibrotactile motor provided vibrations as described in Sec. III-C. The subject was always able to see the operative environment through the standard stereoscopic monitor of the da Vinci system. The orientation of the stick was fully randomized across trials, so that all eighteen possible orientations were tested exactly twelve times and no subject tested the same orientation twice.

The subject performed all four repetitions of a single feedback condition as a block, and the order of the conditions was randomized to test all six possible combinations exactly three times. At the end of each condition, the subject was asked to rate, on two sliders going from 0 to 10, "how easy was it to detect the orientation of the plastic stick?" and "how confident were you in detecting the orientation of the plastic stick?" A score of 0 meant "very difficult" or "not at all confident," and a score of 10 meant "very easy" or "very confident." At the end of the experiment, the subject was asked to choose which feedback conditions were the most and least effective at enabling detection of the plastic stick's orientation. A video of the experiment can be downloaded from http://goo.gl/yrSxa3.

V. Results

To evaluate the subject's performance under each of the considered feedback conditions, we evaluated (1) the absolute error in detecting the orientation of the plastic stick, (2) the

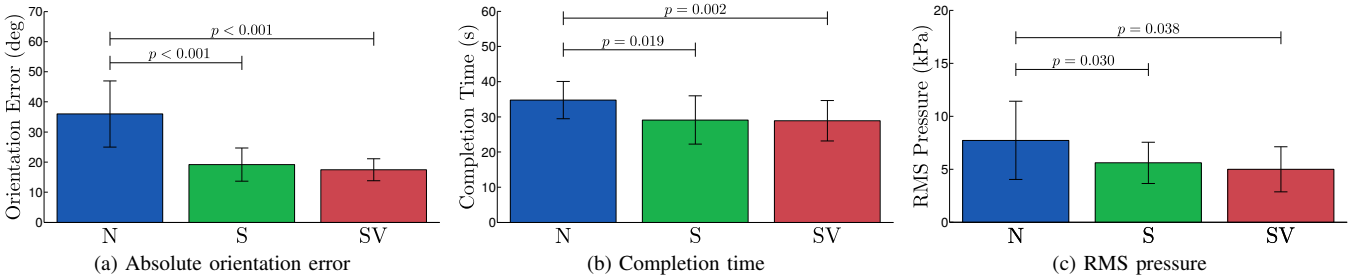

(a) Absolute orientation error (b) Completion time (c) RMS pressure

Fig. 7. Experimental results. Absolute orientation error, completion time, and RMS pressure for conditions providing no force feedback (N), cutaneous feedback by the servo motors (S), and cutaneous feedback by the servo and vibrotactile motors (SV) are plotted (mean and standard deviation). Lower values of these metrics indicate higher performances in completing the palpation task. P-values of post-hoc group comparisons are reported when statistically different.

task completion time, and (3) the root mean square (RMS) pressure exerted by the BioTac on the tissue model. A null value of these three metrics denotes the best performance. Data resulting from different repetitions of the same condition, performed by the same subject, were averaged before comparison with data from the other conditions.

Fig. 7a shows the absolute orientation error results for the three experimental conditions. The collected data passed the Shapiro-Wilk normality test. Mauchly's Test of Sphericity indicated that the assumption of sphericity had been violated ($\chi^2(2) = 6.245, p = 0.044$). A repeated-measures ANOVA with a Greenhouse-Geisser correction showed a statistically significant difference between the means of the three feedback conditions ($F_{1.512,25.696} = 33.890$, $p < 0.001$, a = 0.05). Post-hoc analysis (Games-Howell post-hoc test) revealed statistically significant differences between conditions N and S ($p < 0.001$) and between N and SV ($p < 0.001$). In both cases the errors were lower with haptic feedback.

Fig. 7b shows the completion time results. The collected data passed the Shapiro-Wilk normality test and Mauchly's Test of Sphericity. A repeated-measures ANOVA showed a statistically significant difference between the means of the three feedback conditions ($F_{2,34} = 9.342$, $p = 0.001$, a = 0.05). Post-hoc analysis (Games-Howell post-hoc test) revealed statistically significant differences between conditions N and S ($p = 0.019$) and between N and SV ($p = 0.002$). Completion time was lower with haptic feedback.

Fig. 7c shows the RMS pressure exerted by the BioTac on the tissue model, registered through its DC pressure sensor. The collected data passed the Shapiro-Wilk normality test. Mauchly's Test of Sphericity indicated that the assumption of sphericity had been violated ($\chi^2(2) = 9.120, p = 0.010$). A repeated-measures ANOVA with a Greenhouse-Geisser correction showed a statistically significant difference between the means of the three feedback conditions ($F_{1.394,23.702} = 6.908$, $p = 0.009$, a = 0.05). Post-hoc analysis (Games-Howell post-hoc test) revealed statistically significant differences between conditions N and S ($p = 0.030$) and between N and SV ($p = 0.038$). Exerted pressure was lower with haptic feedback.

Finally, we analyzed the ratings given by the subjects at the end of each feedback condition. Fig. 8 shows the ratings that the three feedback conditions received for the first question ("how easy"). The second question ("how confident") showed similar results (N: 3.45, S: 7.13, SV: 7.71). All of the data

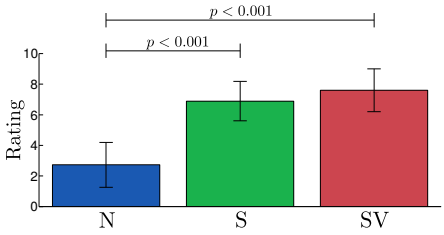

Fig. 8. Experimental results. Preference ratings for the question "How easy was it to detect the orientation of the plastic stick?" are plotted (mean and standard deviation). P-values of post-hoc group comparisons are reported when statistically different.

passed the Shapiro-Wilk normality test and Mauchly's Test of Sphericity. A repeated-measures ANOVA showed a statistically significant difference between the means of the three feedback conditions for both questions ("how easy", $F_{2,34} = 52.460$, $p < 0.001$, a = 0.05; "how confident", $F_{2,34} = 50.517$, $p < 0.001$, a = 0.05). Post-hoc analysis (Games-Howell post-hoc test) revealed statistically significant differences between conditions N and S ($p < 0.001$) and between N and SV ($p < 0.001$) for both questions, with haptic feedback earning higher ratings. The conditions providing cutaneous feedback were also preferred in the post-experimental questionnaire. Eleven subjects chose condition SV as the most effective feedback condition, six subjects chose condition S, and only one chose condition N. All but one considered condition N to be the least effective at enabling detection of the orientation of the plastic stick. The outlier subject who chose condition N as the preferred condition mentioned that he/she considered the cutaneous cues to be somewhat distracting. This subject started the experiment with condition N.

VI. Discussion

Adding cutaneous feedback significantly improved palpation task performance in all of the considered metrics. Moreover, conditions providing cutaneous feedback were highly preferred by the subjects. These results confirm the value of cutaneous feedback in teleoperation and support the validity of the described approach. Interestingly, we did not find any significant differences between the two conditions providing cutaneous feedback, S and SV. Adding vibrations thus did not seem to improve subject performance of the given task.

We believe that this unexpected result stems from the way subjects explored the tissue model. We noticed two different strategies being used during the experiment. Referring to the classification of hand exploratory movements described by Lederman and Klatzky [46], we can describe the first strategy as a "pressure" exploratory movement and the second one as a combination of the "pressure" and the "lateral motion" exploratory movements. We will refer to them as the "pressure strategy" and the "dragging strategy," respectively. A video showing these two exploratory strategies can be downloaded from http://goo.gl/gkdBHc. Eleven subjects used the pressure strategy, and seven used the dragging strategy.

To understand how different strategies affected the performance of the palpation task, we performed a statistical analysis considering only the seven subjects who used the dragging strategy. Fig. 9 shows the absolute orientation error and the mean preference ratings for the three feedback conditions considering only these seven subjects. All of the collected data passed the Shapiro-Wilk normality test. Mauchly's Test of Sphericity indicated that the assumption of sphericity had been violated in the orientation error data ($\chi^2(2) = 7.608, p = 0.022$). A repeated-measures ANOVA showed a statistically significant difference between the means of the three feedback modalities in all of the considered metrics (orientation error, $F_{1.123,6.735}$ = 18.891, $p = 0.003$, a = 0.05; completion time, $F_{2,12}$ = 8.291, $p = 0.005$, a = 0.05; RMS pressure, $F_{2,12}$ = 11.935, $p = 0.001$, a = 0.05). Post-hoc analysis (Games-Howell post-hoc test) revealed statistically significant differences in all metrics between conditions N and S (orientation error, $p = 0.021$; completion time, $p = 0.013$; RMS pressure, $p = 0.015$) and between N and SV (orientation error, $p = 0.011$; completion time, $p = 0.017$; RMS pressure, $p = 0.023$). Conditions S and SV were found to be statistically different only in the orientation error metric ($p = 0.025$), with lower errors occurring when vibrotactile feedback was provided.

Finally, we analyzed the ratings given by the seven dragging subjects at the end of each feedback condition. All of the data passed the Shapiro-Wilk normality test and Mauchly's Test of Sphericity. A repeated-measures ANOVA showed a statistically significant difference between the means of the three feedback conditions for both questions ("how easy", $F_{2,12}$ = 46.790, $p < 0.001$, a = 0.05; "how confident", $F_{2,12}$ = 37.266, $p < 0.001$, a = 0.05). Post hoc analysis with Bonferroni adjustments revealed statistically significant difference between conditions N and S ("how easy", $p = 0.009$; "how confident", $p = 0.008$), and N and SV ($p < 0.001$) for both questions. Conditions S and SV were found to be statistically different in one of the questions ("how easy", $p = 0.009$), with condition SV perceived to be easier. Furthermore, all seven subjects who used the dragging strategy found condition SV to be the most effective at letting them detect the orientation of the plastic stick.

Unlike subjects who used the pressure strategy, the seven subjects who used the dragging strategy were able to take advantage of the vibrotactile feedback provided by our system to improve their detection of the orientation of the hidden plastic stick. These results can be explained by considering

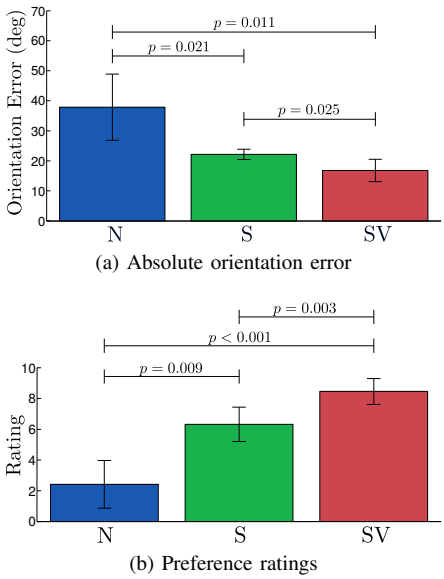

(a) Absolute orientation error

(b) Preference ratings

Fig. 9. Experimental result for the dragging strategy. Absolute orientation error and preference ratings for the question "How easy was it to detect the orientation of the plastic stick?" are plotted (mean and standard deviation), considering only the data from the seven subjects who used the dragging strategy. P-values of post-hoc group comparisons are reported when the differences are statistically significant.

that the vibrotactile feedback may have helped subjects detect the AC pressure transient that occurs when the BioTac moves laterally over an embedded object, a phenomenon documented by other researchers [37]. On the other hand, most of the vibrations generated during the pressure strategy most likely pertained to making and breaking contact with the tissue surface, which is also rendered by the platform's motion, and probably provided little information about the orientation of the hidden stick.

VII. Conclusions

This article presented a novel cutaneous approach to providing haptic feedback for palpation in robot-assisted surgery. The haptic system is composed of a BioTac tactile sensor, in charge of registering fingertip deformations and vibrations at the operating table, and a custom cutaneous feedback device, in charge of applying those deformations and vibrations to the surgeon's fingertip. The BioTac is attached to a da Vinci tool, and the cutaneous device is attached to the robot's corresponding master controller. Contact deformations and vibrations sensed by the BioTac are directly mapped to input commands for the cutaneous device's motors using a model-free algorithm that centers on data collected while the BioTac is inside the cutaneous device. Because no grounded kinesthetic forces are provided to the operator, this haptic feedback approach is inherently stable.

We evaluated the proposed approach in a palpation task using the da Vinci surgical robot. Eighteen subjects were asked to detect the orientation of a plastic stick embedded in a simulated heart tissue model. Providing cutaneous feedback of fingertip deformation significantly improved the task performance in terms of absolute error in detecting the orientation of the plastic stick, completion time, and pressure exerted on the

tissue model. Subjects who used a dragging strategy achieved even better results with cutaneous feedback of fingertip vibrations. Subjects also highly preferred conditions providing cutaneous feedback over the one without any haptic feedback.

VIII. Future Work

In the future, we plan to run a new human subject study enrolling both novices and experienced da Vinci surgeons. This study will let us better understand the importance of cutaneous stimuli at various levels of surgical experience, in addition to its role in the surgeon's learning process. Moreover, we plan to evaluate the proposed rendering approach in other surgery-related tasks, such as suturing and blunt dissection, and to study the possible perceptual interactions between cutaneous feedback of contact deformation and vibration. We also intend to modify the cutaneous feedback device to use continuous rotation servos, add a force sensor on the platform, and make its overall design and form factor smaller and more comfortable. The new servos would enable the device to reach a larger range of platform orientations, and the force sensor would enable us to automatically re-calibrate the algorithm for different fingertip sizes, improving the quality of the tactile rendering across individuals. We will also test whether palpation sensations could be conveyed more effectively using alternative mobile platform designs, such as ones that include pneumatic balloons or other non-rigid elements.

Finally, we intend to investigate the practical translational aspects of the proposed cutaneous system. The BioTac sensor cannot be used during surgery in its current form. It is too large to fit through a keyhole incision, it has exposed electrical connections, and it is not sterilizable. A modified version of the BioTac suitable for surgery would need to be small enough to be inserted through a trocar. The back of the sensor would need to include features that would enable it to be held by or attached to a surgical instrument. The electrical connections between the sensor and the cord would need to be redesigned to electrically insulate all wires and connections. Furthermore, a sterilization method would need to be developed to thoroughly disinfect the cord and the core part of the BioTac between patients; while the standard approach of steam sterilization would damage the plastic and the electronics, a BioTac could probably be sterilized using ethylene oxide gas or another low-temperature sterilization technique. The external rubber skin and the saline solution with which the skin is filled could both be made sterile and disposable. Despite these required improvements to the sensor, the presented cutaneous rendering algorithm is quite general, and it should work in any scenario where similar sensing and actuation systems can be employed. Any modification to the sensor aimed at improving its applicability in surgery would thus not require any major change in the rendering algorithm and experimental protocol.

Acknowledgment

The authors thank Ian McMahon and Jacqueline Koehn for helping set up the BioTac sensing system, Priyanka Shirsat for helping build the cutaneous device, Alexis Block for helping create the tissue models, and Intuitive Surgical, Inc., for donating the da Vinci Standard.

References

[1] T. B. Sheridan, "Telerobotics," *Automatica*, vol. 25, no. 4, pp. 487–507, 1989.

[2] ——, *Telerobotics, automation, and human supervisory control*. The MIT Press, 1992.

[3] N. Diolaiti *et al.*, "Stability of haptic rendering: Discretization, quantization, time delay, and Coulomb effects," *IEEE Transactions on Robotics*, vol. 22, no. 2, pp. 256–268, 2006.

[4] D. Prattichizzo, C. Pacchierotti, and G. Rosati, "Cutaneous force feedback as a sensory subtraction technique in haptics," *IEEE Transactions on Haptics*, vol. 5, no. 4, pp. 289–300, 2012.

[5] A. M. Okamura, "Methods for haptic feedback in teleoperated robot-assisted surgery," *Industrial Robot: An International Journal*, vol. 31, no. 6, pp. 499–508, 2004.

[6] ——, "Haptic feedback in robot-assisted minimally invasive surgery," *Current opinion in urology*, vol. 19, no. 1, p. 102, 2009.

[7] E. Westebring-Van Der Putten *et al.*, "Haptics in minimally invasive surgery-a review," *Minimally Invasive Therapy & Allied Technologies*, vol. 17, no. 1, pp. 3–16, 2008.

[8] O. Van der Meijden and M. Schijven, "The value of haptic feedback in conventional and robot-assisted minimal invasive surgery and virtual reality training: a current review," *Surgical Endoscopy*, vol. 23, no. 6, pp. 1180–1190, 2009.

[9] A. Wedmid, E. Llukani, and D. I. Lee, "Future perspectives in robotic surgery," *BJU International*, vol. 108, no. 6b, pp. 1028–1036, 2011.

[10] S. E. Salcudean, S. Ku, and G. Bell, "Performance measurement in scaled teleoperation for microsurgery," in *Proc. First Joint Conference on Computer Vision, Virtual Reality and Robotics in Medicine and Medial Robotics and Computer-Assisted Surgery*, 1997, pp. 789–798.

[11] A. Kazi, "Operator performance in surgical telemanipulation," *Presence: Teleoperators & Virtual Environments*, vol. 10, no. 5, pp. 495–510, 2001.

[12] L. Moody *et al.*, "Objective surgical performance evaluation based on haptic feedback," *Studies in Health Technology and Informatics*, pp. 304–310, 2002.

[13] C. W. Kennedy *et al.*, "A novel approach to robotic cardiac surgery using haptics and vision," *Cardiovascular Engineering*, vol. 2, no. 1, pp. 15–22, 2002.

[14] A. Pillarisetti *et al.*, "Evaluating the effect of force feedback in cell injection," *IEEE Transactions on Automation Science and Engineering*, vol. 4, no. 3, pp. 322–331, 2007.

[15] B. Hannaford *et al.*, "Performance evaluation of a six-axis generalized force-reflecting teleoperator," *IEEE Transactions on Systems, Man, and Cybernetics*, vol. 21, no. 3, pp. 620–633, 1991.

[16] M. J. Massimino and T. B. Sheridan, "Teleoperator performance with varying force and visual feedback," *Human Factors: The Journal of the Human Factors and Ergonomics Society*, vol. 36, no. 1, pp. 145–157, 1994.

[17] C. R. Wagner, N. Stylopoulos, and R. D. Howe, "The role of force feedback in surgery: analysis of blunt dissection," in *Proc. 10th Symposium of Haptic Interfaces for Virtual Environment and Teleoperator Systems*, 2002, pp. 68–74.

[18] D. Prattichizzo *et al.*, "Using a fingertip tactile device to substitute kinesthetic feedback in haptic interaction," *Haptics: Generating and Perceiving Tangible Sensations*, pp. 125–130, 2010.

[19] C. Pacchierotti *et al.*, "Two finger grasping simulation with cutaneous and kinesthetic force feedback," *Haptics: Perception, Devices, Mobility, and Communication*, pp. 373–382, 2012.

[20] L. Meli, C. Pacchierotti, and D. Prattichizzo, "Sensory subtraction in robot-assisted surgery: fingertip skin deformation feedback to ensure safety and improve transparency in bimanual haptic interaction," *IEEE Transactions on Biomedical Engineering*, vol. 61, no. 4, pp. 1318–1327, 2014.

[21] R. E. Schoonmaker and C. G. L. Cao, "Vibrotactile force feedback system for minimally invasive surgical procedures," in *Proc. of IEEE International Conference on Systems, Man and Cybernetics*, vol. 3, 2006, pp. 2464–2469.

[22] W. B. Griffin, W. R. Provancher, and M. R. Cutkosky, "Feedback strategies for telemanipulation with shared control of object handling forces," *Presence: Teleoperators and Virtual Environments*, vol. 14, no. 6, pp. 720–731, 2005.

[23] M. Kitagawa *et al.*, "Effect of sensory substitution on suture-manipulation forces for robotic surgical systems," *Journal of Thoracic and Cardiovascular Surgery*, vol. 129, no. 1, pp. 151–158, 2005.
[24] I. Birznieks *et al.*, "Encoding of direction of fingertip forces by human tactile afferents," *The Journal of Neuroscience*, vol. 21, no. 20, pp. 8222–8237, 2001.
[25] K. O. Johnson, "The roles and functions of cutaneous mechanoreceptors," *Current Opinion in Neurobiology*, vol. 11, no. 4, pp. 455–461, 2001.
[26] W. McMahan *et al.*, "Tool contact acceleration feedback for telerobotic surgery," *IEEE Transactions on Haptics*, vol. 4, no. 3, pp. 210–220, 2011.
[27] C.-H. King *et al.*, "Tactile feedback induces reduced grasping force in robot-assisted surgery," *IEEE Transactions on Haptics*, vol. 2, no. 2, pp. 103–110, 2009.
[28] ——, "A multielement tactile feedback system for robot-assisted minimally invasive surgery," *IEEE Transactions on Haptics*, vol. 2, no. 1, pp. 0052–56, 2009.
[29] M. Li *et al.*, "Haptics for multi-fingered palpation," in *Proc. IEEE International Conference on Systems, Man, and Cybernetics*, 2013, pp. 4184–4189.
[30] A. Stanley and A. Okamura, "Controllable surface haptics via particle jamming and pneumatics," *IEEE Transactions on Haptics*, vol. 8, no. 2, pp. 20–30, 2015.
[31] M. Li *et al.*, "Multi-fingered haptic palpation utilizing granular jamming stiffness feedback actuators," *Smart Materials and Structures*, vol. 23, no. 9, p. 095007, 2014.
[32] D. A. Kontarinis and R. D. Howe, "Tactile display of vibratory information in teleoperation and virtual environments," *Presence: Teleoperators and Virtual Environments*, vol. 4, no. 4, pp. 387–402, 1995.
[33] J. K. Koehn and K. J. Kuchenbecker, "Surgeons and non-surgeons prefer haptic feedback of instrument vibrations during robotic surgery," accepted for publication in *Surgical Endoscopy*.
[34] C. Pacchierotti, D. Prattichizzo, and K. J. Kuchenbecker, "A data-driven approach to remote tactile interaction: from a BioTac sensor to any fingertip cutaneous device," in *Proc. of Eurohaptics*, Versailles, France, 2014.
[35] ——, "Displaying sensed tactile cues with a fingertip haptic device," *IEEE Transactions on Haptics, In Press*, 2015.
[36] N. Wettels and G. E. Loeb, "Haptic feature extraction from a biomimetic tactile sensor: force, contact location and curvature," in *Proc. IEEE International Conference on Robotics and Biomimetics*, 2011, pp. 2471–2478.
[37] M. S. Arian *et al.*, "Using the BioTac as a tumor localization tool," in *Proc. IEEE Haptics Symposium*, Feb. 2014, pp. 443–448.
[38] W. R. Provancher *et al.*, "Contact location display for haptic perception of curvature and object motion," *International Journal of Robotics Research*, vol. 24, no. 9, pp. 691–702, Sep. 2005.
[39] L. Wauben *et al.*, "Application of ergonomic guidelines during minimally invasive surgery: a questionnaire survey of 284 surgeons," *Surgical Endoscopy And Other Interventional Techniques*, vol. 20, no. 8, pp. 1268–1274, 2006.
[40] E. H. Lawson *et al.*, "Postural ergonomics during robotic and laparoscopic gastric bypass surgery: a pilot project," *Journal of Robotic Surgery*, vol. 1, no. 1, pp. 61–67, 2007.
[41] D. Prattichizzo *et al.*, "Towards wearability in fingertip haptics: a 3-dof wearable device for cutaneous force feedback," *IEEE Transactions on Haptics*, vol. 6, no. 4, pp. 506–516, 2013.
[42] C. Pacchierotti, A. Tirmizi, and D. Prattichizzo, "Improving transparency in teleoperation by means of cutaneous tactile force feedback," *ACM Transactions on Applied Perception*, vol. 11, no. 1, pp. 4:1–4:16, 2014.
[43] D. M. Mount and S. Arya, "ANN: A Library for Approximate Nearest Neighbor Searching," http://www.cs.umd.edu/~mount/ANN/, 2010.
[44] A. V. Oppenheim *et al.*, *Discrete-time signal processing*. Prentice-hall Englewood Cliffs, 1989, vol. 2.
[45] T. Yamamoto *et al.*, "Tissue property estimation and graphical display for teleoperated robot-assisted surgery," in *IEEE International Conference on Robotics and Automation*, 2009, pp. 4239–4245.
[46] S. J. Lederman and R. L. Klatzky, "Hand movements: A window into haptic object recognition," *Cognitive Psychology*, vol. 19, no. 3, pp. 342–368, 1987.

Claudio Pacchierotti (S'12) received the B.S., M.S., and Ph.D. degrees from the University of Siena, Italy in 2009, 2011, and 2014, respectively. He was an exchange student at the Karlstad University, Sweden in 2010. He spent the first seven months of 2014 visiting the Penn Haptics Group at the University of Pennsylvania, Philadelphia, USA, which is part of the General Robotics, Automation, Sensing, and Perception (GRASP) Laboratory. He also visited the Dept. of Innovation in Mechanics and Management of the University of Padua and the Institute for Biomedical Technology and Technical Medicine (MIRA) of the University of Twente in 2013 and 2014, respectively. He received the 2014 EuroHaptics Best PhD Thesis Award for the best doctoral thesis in the field of haptics. He is currently a postdoctoral researcher at the Dept. of Advanced Robotics of the Italian Institute of Technology, Genova, Italy. His research deals with robotics and haptics, focusing on cutaneous force feedback techniques, wearable devices, and haptics for robotic surgery.

Domenico Prattichizzo (S'93 – M'95) eceived the Ph.D. degree in Robotics and Automation from the University of Pisa in 1995. Since 2002 he is an Associate Professor of Robotics at the University of Siena and since 2009 he is a Scientific Consultant at Istituto Italiano di Tecnoloogia. In 1994, he was a Visiting Scientist at the MIT AI Lab. Since 2014, he is Associate Editor of Frontiers of Biomedical Robotics. From 2007 to 2013 he has been Associate Editor in Chief of the IEEE Transactions on Haptics. From 2003 to 2007, he has been Associate Editor of the IEEE Transactions on Robotics and IEEE Transactions on Control Systems Technologies. He has been Chair of the Italian Chapter of the IEEE RAS (2006-2010), awarded with the IEEE 2009 Chapter of the Year Award. Research interests are in haptics, grasping, visual servoing, mobile robotics and geometric control. He is currently the Coordinator of the IP collaborative project "WEARable HAPtics for Humans and Robots" (WEARHAP).

Katherine J. Kuchenbecker (S'04 – M'06) received the B.S., M.S., and Ph.D. degrees in mechanical engineering from Stanford University, Stanford, CA, in 2000, 2002, and 2006, respectively. She completed a Postdoctoral Research Fellowship at the Johns Hopkins University, Baltimore, MD, in 2006–2007. She is currently an Associate Professor in Mechanical Engineering and Applied Mechanics at the University of Pennsylvania, Philadelphia. Her research centers on the design and control of haptic interfaces and robotic systems, and she directs the Penn Haptics Group, which is part of the General Robotics, Automation, Sensing, and Perception (GRASP) Laboratory. Prof. Kuchenbecker was the recipient of the 2009 National Science Foundation CAREER Award, the 2008 and 2011 Citations for Meritorious Service as a Reviewer for the IEEE Transactions on Haptics, and the 2012 IEEE Robotics and Automation Society Academic Early Career Award. She is co-chairing the IEEE Haptics Symposium in 2016 and 2018, and she is presently a co-chair of the IEEE RAS Technical Committee on Haptics.